Available online at www.sciencedirect.com

SciVerse ScienceDirect

Ceramics International 38 (2012) 3465–3472

CERAMICS INTERNATIONAL

www.elsevier.com/locate/ceramint

Dielectric evaluation of electrically tunable $Ba_{0.6}Sr_{0.4}TiO_3$ thick films prepared by screen printing

Xiao-Fei Zhang [a,b], Qing Xu [a,*], Di Zhan [a], Han-Xing Liu [a], Wen Chen [a], Duan-Ping Huang [a]

[a] School of Materials Science and Engineering, Wuhan University of Technology, Wuhan 430070, People's Republic of China
[b] School of Mathematics and Physics, Huangshi Institute of Technology, Huangshi 435003, People's Republic of China

Received 29 October 2011; received in revised form 20 December 2011; accepted 21 December 2011
Available online 12 January 2012

Abstract

$Ba_{0.6}Sr_{0.4}TiO_3$ thick films were prepared on alumina substrates by screen printing using superfine starting powder derived from a citrate method. The thick film sintered at 1250 °C showed a cubic perovskite structure and a porous microstructure. The dielectric properties of the thick film were investigated in comparison with dense ceramic specimen. The comparison indicates a significant effect of the porous microstructure on the dielectric properties. The porous microstructure of the thick film resulted in a lowered dielectric constant, an increased dielectric loss and a reduction of field history dependence for the dielectric nonlinearity under bias electric field. The increased dielectric dissipation of the thick film was interpreted with an appreciable interfacial polarization and an enhanced electric conduction. Compared with the ceramic specimen, the porous thick film maintained a reasonably good dielectric nonlinearity because of a large phenomenological coefficient. At room temperature, the thick film attained a dielectric constant of 1270 and a dielectric loss of 1.4% at zero bias field and 10 kHz together with a tunability of 60% and a figure of merit of 43 at 57 kV/cm and 10 kHz.

Keywords: B. Microstructure-final; B. Porosity; C. Dielectric properties; D. Perovskites

1. Introduction

Barium strontium titanate ($Ba_{1-x}Sr_xTiO_3$, BST) exhibits strong dielectric nonlinearity under bias electric field and adjustable Curie temperatures. The desired properties make the dielectrics a promising candidate material for electrically tunable microwave devices. The application of BST in the tunable microwave devices has been explored in various material forms, including bulk ceramics, thin films and thick films [1,2]. BST thick films allow low fabrication costs compared with the thin films and small bias voltages required for tuning relative to the bulk ceramics. Moreover, the thick film application accommodates the demands of miniaturization, complexity and multilayer assembles, which emerge as the mainstream of electronic components. Fabricating BST thick films on alumina substrates by screen printing has been believed to be cost-effective in view of mass production [3,4]. An additional advantage of the technique is its flexibility in producing the thick films with complicated and diversified patterns.

The BST thick films, unfortunately, suffer from severe reactions with the substrates at high sintering temperatures [3,5]. Thus, the sintering temperatures of the thick films have to be limited to less than 1250 °C. This led to a porous microstructure and an unsatisfactory adhesion to the substrates for the thick films [5]. Adding sintering aids, such as glass frits [5,6] or oxide additives [7], is an usually employed and viable strategy to overcome the problem. Nevertheless, the reactions between the BST thick films and the sintering aids may result in unfavorable changes in the structure and dielectric properties [6]. Preparing BST thick films from highly reactive powders is expected to be an alternative approach to improve the sintering of the thick films. On the other hand, porous BST thick films displayed some dielectric behaviors distinct from their dense ceramic counterparts [7,8]. From a microstructural viewpoint, main difference between the BST of the two forms lies in densification degree. In this sense, taking a deep insight into the dielectric properties of the thick films in relation to their porous microstructures appears to be necessary.

* Corresponding author. Tel.: +86 27 87863277; fax: +86 27 87864580.
E-mail address: xuqing@whut.edu.cn (Q. Xu).

0272-8842/$36.00
doi:10.1016/j.ceramint.2011.12.060

We synthesized superfine $Ba_{0.6}Sr_{0.4}TiO_3$ powder by a citrate method and achieved ceramic specimens with reasonable densification (about 95%) by sintering at 1260 °C [9]. The dielectric nonlinearity of the ceramics under bias electric field was studied [10]. As a continuous effort, we prepared $Ba_{0.6}Sr_{0.4}TiO_3$ thick films on alumina substrates by screen printing using the superfine powder. In this work, we investigate the dielectric properties of the thick films as a function of temperature, frequency and applied electric field. The research was conducted in comparison with the dense $Ba_{0.6}Sr_{0.4}TiO_3$ ceramics.

2. Experimental

$Ba_{0.6}Sr_{0.4}TiO_3$ powder was synthesized by a citrate method. The synthesized powder had a single perovskite phase and superfine particle morphology (around 100 nm). The synthesis and characterization of the powder have been reported elsewhere [9]. Think film capacitors with $Ba_{0.6}Sr_{0.4}TiO_3$ as the dielectric layer were prepared on 96% aluminum substrates by screen printing. Platinum and silver were adopted as the bottom and top electrodes, respectively. The ink for screen printing was prepared by mixing the synthesized powder with organic medium at a solid loading of 65 wt.%. The organic medium was composed of ethyl cellulose (5 wt.%), terpinol (65 wt.%), n-butanol (10 wt.%), di-n-butyl phthalate (10 wt.%) and 2-butoxyethanol acetate (10 wt.%). Platinum paste was screen printed onto the aluminum substrate and sintered at 1350 °C for 2 h. Then the ink was printed on the bottom electrode and calcined at 600 °C for 1 h. This procedure was repeated twice. Afterwards, the thick film was sintering at 1250 °C for 2 h in air. Finally, sliver paste was printed on the thick film and sintered at 850 °C for 0.5 h. For comparison purposes, $Ba_{0.6}Sr_{0.4}TiO_3$ ceramics were prepared from the synthesized powder by sintering at 1260 °C for 2 h. The preparation and dielectric properties of the ceramics have been previously reported [10].

The phase structure of the specimens was examined by a Philips X'pert PBO X-ray diffractometer using Cu Kα radiation. The microstructure of the specimens was observed at a JEOL JSM-5610LV scanning electron microscope (SEM). The microstructural parameters of the specimens were determined from observed SEM images using the Image Profession Plus software. The porosity of the thick films was estimated by counting black and gray pixels of the SEM images, which refer to pores and grains, respectively [11]. The dielectric properties of the thick films were measured based on the thick film capacitors. The dielectric constant (ε_r) and the loss (tan δ) were measured by a TH2828 precision LCR meter and a SSC-M10 environmental chamber (C4 controller) in the range of 20 Hz to 1 MHz between −80 and 130 °C. The polarization (P) versus electric field (E) relation of the specimens was measured at room temperature (25 °C) by a Radiant precision workstation based on the Sawyer-Tower circuit at 50 Hz. The leakage current data were also measured at the apparatus as a function of applied electric field. The nonlinear dielectric properties of the thick films were measured at room temperature by a TH2818 automatic component analyzer at 10 kHz under bias electric fields forward sweeping from 0 kV/cm to 57 kV/cm. A blocking circuit was adopted to protect the analyzer from the applied bias voltages. Dielectric data were recorded after holding at each applied bias field for 10 s. To examine the dependence of the dielectric properties on history of the bias filed, the dielectric constant of the thick films was measured in continuous cycles of bias field sweep. In each cycle, the bias fields were forward swept from zero to 57 kV/cm and then backward swept to zero kV/cm. The measurement was continuously performed for 11 cycles.

3. Results and discussion

3.1. Structural characterization

Fig. 1 shows the X-ray diffraction (XRD) patterns of the ceramic specimen and the thick film without the top electrode. A perovskite structure with a cubic symmetry was readily identified for the ceramic specimen [10]. In addition to a cubic perovskite phase, platinum and aluminum phases were also detected for the thick film, which are believed to be caused by the bottom electrode and the substrate, respectively. A closer look indicated that, compared with the ceramic specimen, the XRD peaks corresponding to the perovskite phase of the think film slightly shifted toward lower diffraction angle directions. This implies an increased size of the unit cell for the perovskite structure of the thick film.

Fig. 2 shows the SEM images of the ceramic specimen and the thick film without the top electrode. The ceramic specimen exhibited a dense microstructure with average grain size of 0.5 μm (Fig. 2a). The Archimedes measurement indicated that the ceramic specimen attained nearly 95% of the theoretical density [9]. The surface and cross-section views of the thick film illustrate a porous microstructure (Fig. 2b and c). From the surface and cross-section views, the porosity of the thick film was estimated to be 19% and 20%, respectively. The average gain size of the thick film was determined to be 0.7 μm, which

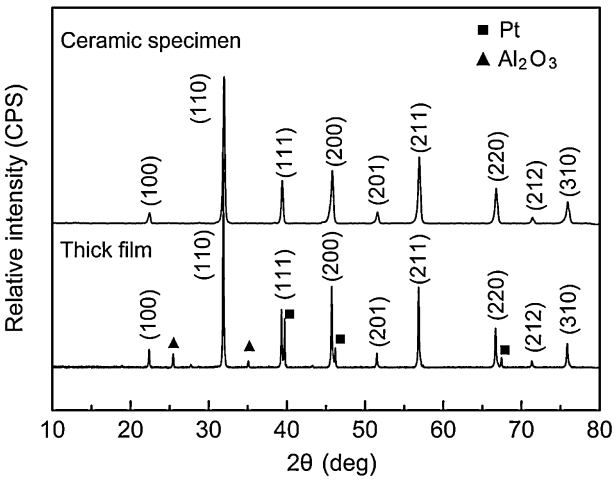

Fig. 1. XRD patterns of the ceramic specimen and the thick film without the top electrode.

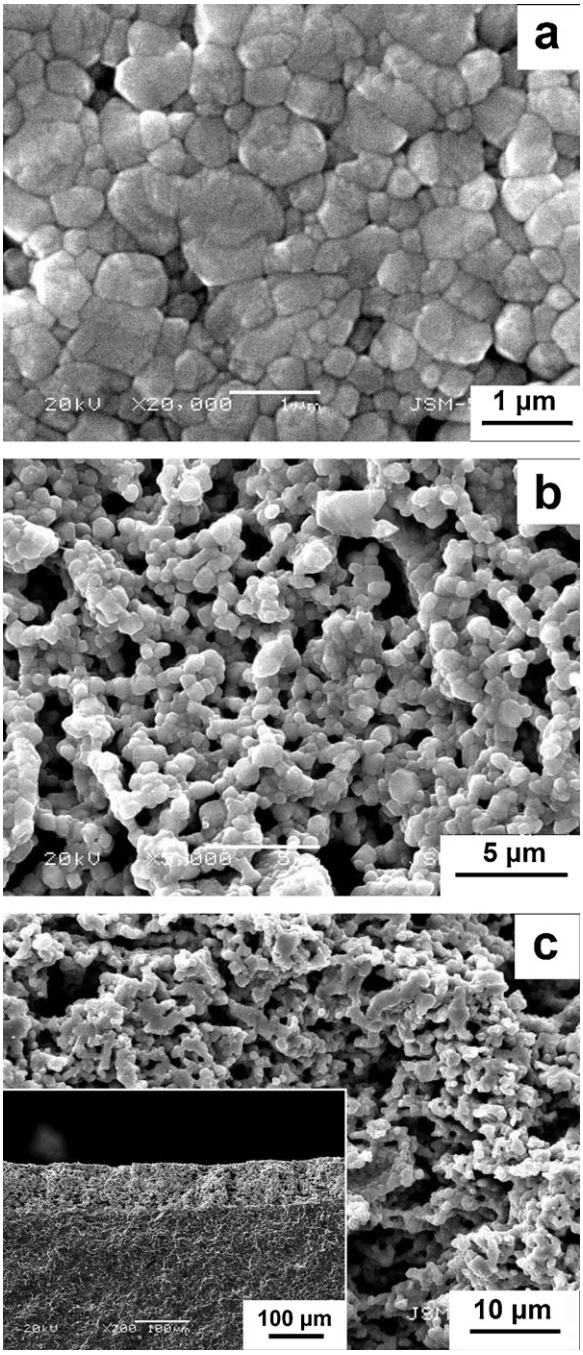

Fig. 2. SEM images of (a) the ceramic specimen, (b) surface view and (c) cross-section view of the thick film without the top electrode. The inset in Fig. 3c shows a panoramic view of the cross-section of the thick film.

is larger than that of the ceramic specimen. The inset in Fig. 2c provides a panoramic view for the cross-section of the thick film, showing a generally uniform thickness of about 70 μm and a good adhesion to the matrix.

3.2. Dielectric behavior as a function of temperature and frequency

Fig. 3 shows the temperature dependence of the dielectric constant and the loss of the thick film measured at different

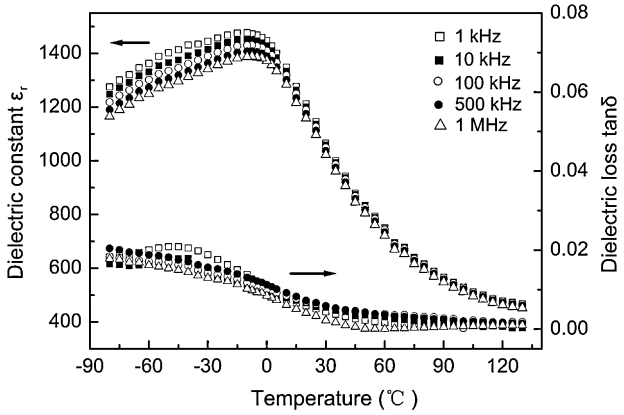

Fig. 3. Temperature dependence of the dielectric constant and the loss of the thick film measured at different frequencies.

frequencies. For each frequency, the dielectric constants presented a broad peak at around −2.5 °C, which is well consistent with the result of the ceramic specimen [10]. As well known, the dielectric anomaly corresponds to a ferroelectric–paraelectric phase transition. The XRD analysis (Fig. 1) and the dielectric inspection suggest a macroscopically paraelectric state for the thick film at room temperature. It was noticed that the dielectric constants showed a frequency dispersion in low temperature region. This behavior is discrepant from the case of $Ba_{0.6}Sr_{0.4}TiO_3$ ceramics. It has been well established that the dielectric constants of $Ba_{0.6}Sr_{0.4}TiO_3$ ceramics are basically frequency-independent [10,12]. The discrepancy infers a difference in polarization mechanism between the thick film and ceramic specimen. The difference is assumed to be related to the porous microstructure of the thick film. Moreover, the frequency dispersion of the dielectric constant turned to be nearly vanished after about 10 °C. The dielectric loss offered an analogous variation, with the frequency dispersion of the parameter becoming obscure at higher temperatures above 90 °C.

Fig. 4 shows the frequency spectra of the dielectric constant and the loss measured at different temperatures for the ceramic specimen and the thick film. At room temperature (20 °C), the dielectric constant and the loss of the ceramic specimen displayed a flat change with frequency (Fig. 4a), whereas those of the thick film significantly varied (Fig. 4b). Especially, the two dielectric parameters of the thick film sharply increased with deceasing frequency in the range of 20 Hz to 1 kHz. This behavior is reminiscent of the Maxwell–Wagner effect, implying the existence of interfacial polarization in the thick film [13,14]. The interfacial polarization can be attributed to a charge accumulation at the grain boundaries [8]. The frequency dispersion of the dielectric properties in Fig. 3 is also presumed to be related to the interfacial polarization. At elevated temperatures, the spectra of the dielectric loss of the thick film showed a decayed Maxwell–Wagner effect, while the variation of the dielectric constant with frequency became minor (Fig. 4c and d). This phenomenon suggests that the dielectric loss is more useful in diagnosing the interfacial polarization. The suggestion is consistent with literature result [14]. Moreover, peaks of the dielectric loss appeared at about 50 Hz. This result

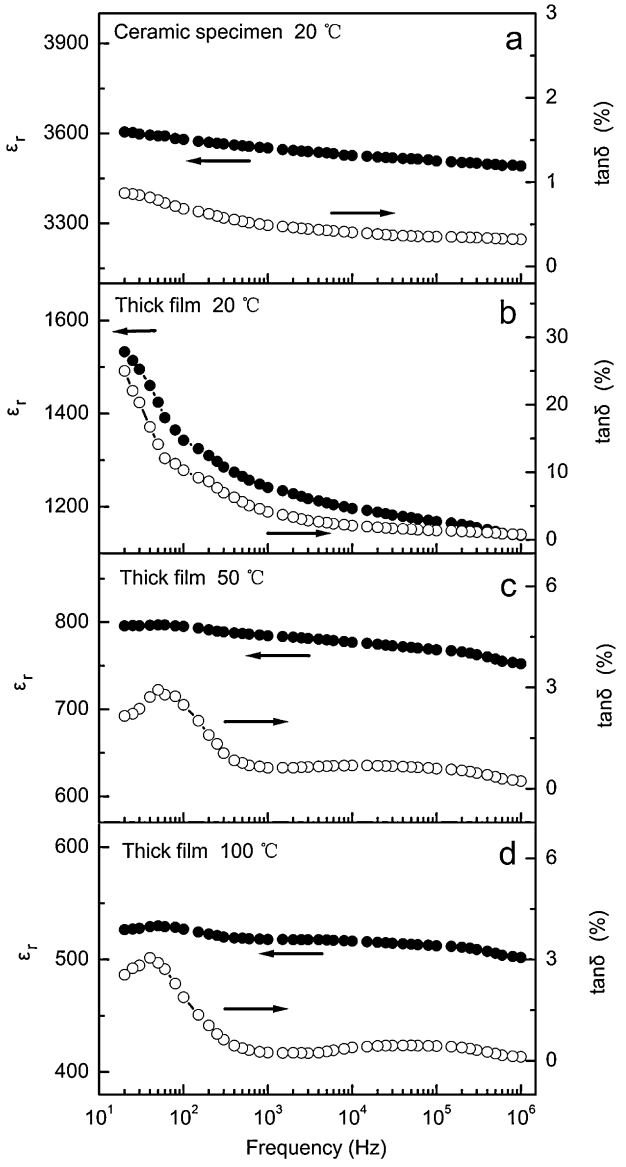

Fig. 4. Frequency spectra of the dielectric constant and the loss measured at different temperatures for the ceramic specimen and the thick film.

indicates shorter relaxation times for the interfacial polarization at the elevated temperatures compared with the case of at room temperature.

The interfacial polarization of the thick film can be tentatively interpreted in relation to its porous microstructure. As is well known, the lattice oxygen of BST perovskites is volatilizable at high temperatures. Presence of oxygen vacancies caused by intrinsic oxygen loss and their effects on various properties have been reported for BST ceramics sintered at different temperatures (≥1200 °C) [15–17]. The formation of oxygen vacancies and their ionization can be described by the following equations in the Kröger–Vink notation:

$$O_O^{\times} \rightarrow 2V_O^{\bullet\bullet} + \tfrac{1}{2}O_2 + 2e' \quad (1)$$

$$2Ti_{Ti}^{\times} + 2e' \rightarrow 2Ti_{Ti}' \quad (2)$$

As afore-mentioned, the ceramic specimen attained about 95% of the theoretical density after sintering at 1260 °C. Due to the reasonably good densification, the formation of oxygen vacancies in the ceramic bulk during the sintering involved oxygen diffusion from the interior to the surface. On the contrary, the porous microstructure of the thick film means that large amounts of the grains are exposed in air. This led to a fast kinetics for the generation of oxygen vacancies in the thick film during sintering. In other words, the porous thick film sintered at 1250 °C experienced more pronounced lattice oxygen loss than the dense ceramic specimen sintered at 1260 °C. This case resulted in higher concentrations of oxygen vacancies and reduced titanium ions in the lattice of the thick film. The higher concentration of reduced titanium ions in the thick film is regarded to be responsible for the larger unite cell of its perovskite structure (Fig. 1). The higher concentration of oxygen vacancies is favorable to mass transport and grain growth during sintering. This effect is believed to account for the larger grain size of the thick film (Fig. 2).

Furthermore, there should be a distribution in concentration of oxygen vacancies for the grains of the thick film. From a dynamic viewpoint, the concentration of oxygen vacancies on the outer surfaces of the exposed grains should be higher compared to the case of in the grain-interiors [18]. The positively charged oxygen vacancies ($V_O^{\bullet\bullet}$) on the surfaces of the grains are ready to be trapped by the grain boundaries. To maintain charge neutrality, a segregation of the negatively charged Ti_{Ti}' to the grain boundaries is plausible. Accordingly, a charge accumulation was created at the grain boundaries. This picture is proposed to the scenario to explain the interfacial polarization in the thick film.

The evolution of the dielectric spectra with temperature (Fig. 4b–d) suggests a thermally activated effect on the interfacial polarization. On one hand, the oxygen vacancies localized at the grain boundaries can be thermally activated to migrate at elevated temperatures. This case decreased the charge polarization at the grain boundaries and, as a result, reduced the Maxwell–Wagner effect. On the other hand, elevating temperature enhanced the mobility of the charged defects accumulating at the grain boundaries, facilitating the response of the interfacial polarization to input ac signals of the dielectric measurement. This case is proposed to be responsible for the shorter relaxation times of the interfacial polarization at the elevated temperatures (Fig. 4c and d). The thermally activated effect is also believed to be the cause for the variation of the frequency dispersion of the dielectric properties with temperature in Fig. 3.

3.3. Polarization and leakage current as a function of applied electric field

Fig. 5 shows the *P–E* relation of the ceramic specimen and the thick film measured at room temperature. The slim hysteresis loop of the ceramic specimen suggests the existence of the polar nano-regions (PNRs) embedded in the paraelectric background [10]. The loop of the thick film became smeared. This is attributed to its porous microstructure. Moreover, the

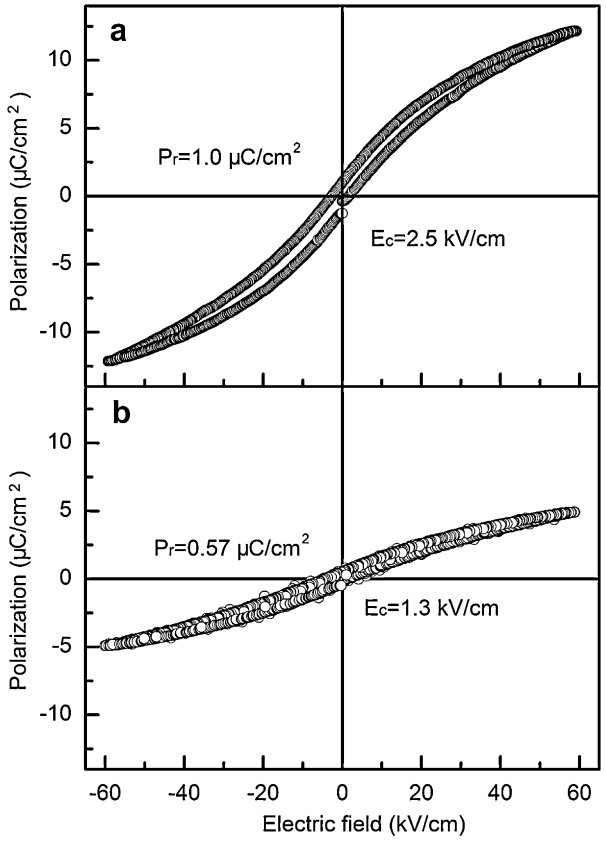

Fig. 5. *P–E* loops measured at room temperature for (a) the ceramic specimen and (b) the thick film.

measured data of the thick film is apparently bouncing. This suggests relatively large leakage currents under the applied electric fields for the thick film.

Fig. 6 shows the leakage current as a function of applied electric field for the ceramic specimen and the thick film at room temperature. The leakage currents of the two specimens exhibited a nonlinear variation with applied electric field. Within the range of 1–5 kV/cm, the leakage currents of the thick film increased by three orders of magnitude. The tunneling behavior is in agreement with the picture of the interfacial polarization [19]. On comparison, the nonlinear behavior of the ceramic specimen is less pronounced. Within the most range of the applied electric fileds (>5 kV/cm), the leakage currents of the thick film are larger by one order of magnitude than the ceramic specimen. The large leakage current of the thick film can be explained with the generation of large amounts of oxygen vacancies and reduced titanium ions. The electrons weakly bounded by Ti^{4+} (Eq. (2)) can be easily thermally activated and become conducting carriers [20].

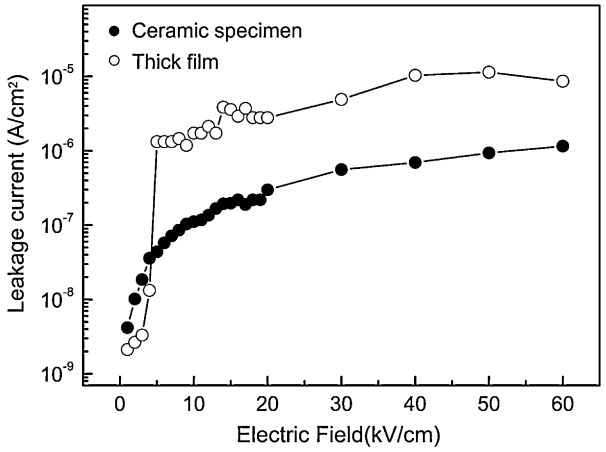

Fig. 6. Leakage current as a function of applied electric field for the ceramic specimen and the thick film at room temperature.

3.4. Dielectric nonlinearity under bias electric field

Fig. 7 shows the dielectric properties of the thick film as a function of bias electric field. The decline of the dielectric constant and the loss with increasing bias electric field substantiates the dielectric nonlinearity of the thick film. Compared with the data of the ceramic specimen ($\varepsilon_r = 3500$, $\tan\delta = 0.48\%$) [10], the dielectric constant (1270) of the thick film at zero bias field is lowered by almost two times and the loss (1.4%) is increased by nearly two folds. The lowered dielectric constant is believed to be due to the porous microstructure of the thick film. The increased dielectric loss is ascribed to two reasons. One is the dissipation arising from the response of the interfacial polarization to ac signals of the dielectric measurement [19]. Another is an enhanced conduction loss resulting from the transport of electric carriers [7,21]. As can be noticed, both of the reasons are related with the porous microstructure of the thick film.

The tunability of the thick film attained 35% and 60% at 21 and 57 kV/cm, respectively. The former value is comparable with the results (30–34%) measured at 30 kV/cm for Li_2O-added $Ba_{0.55}Sr_{0.45}TiO_3$ thick films sintered at low temperatures [7], while the latter is competitive to those (45–70%) measured

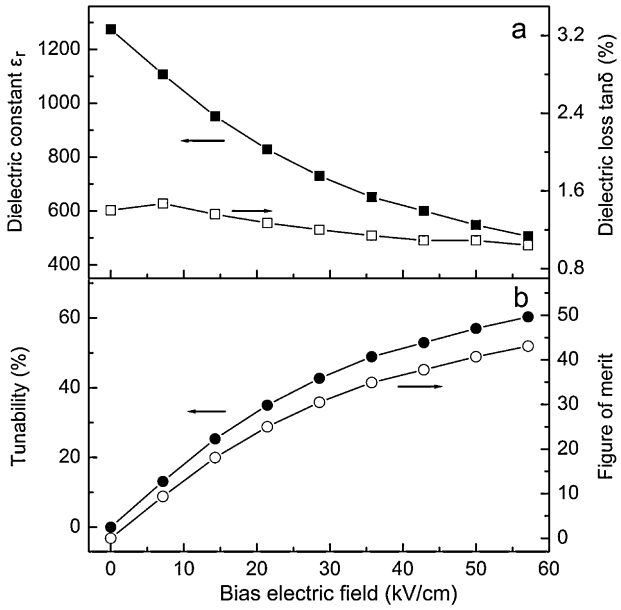

Fig. 7. Nonlinear dielectric properties of the thick film as a function of bias electric field.

at the bias fields above 110 kV/cm for $Ba_{0.6}Sr_{0.4}TiO_3$ thick films with varied porosities [3]. Despite an apparently lowered dielectric constant, the tunability (35%) of the thick film measured at 21 kV/cm is fairly close to that (39%) of the ceramic specimen measured at 20 kV/cm [10]. This result is similar to that of previous literature, where porous $Ba_{0.5}Sr_{0.5}TiO_3$ ceramics with significantly varied porosities (5–28.8%) and dielectric constants (990–1690) showed nearly invariant tunabilities (17.6–19.6% at 26 kV/cm) [22]. The thick film achieved figure of merits (FOM, defined as the ratio of the tunability to the dielectric loss at zero bias field) of 25 and 43 at 21 and 57 kV/cm, respectively. The FOM determined at 21 kV/cm is analogous to literature result (22.2) for $Ba_{0.6}Sr_{0.4}TiO_3$ thick film obtained at 20 kV/cm [23].

The dielectric constants of the thick film measured from continuous cycles of bias electric field sweep were fitted to the Johnson's phenomenological relation, as depicted by the following equation [24]:

$$\frac{\varepsilon_{r(E)}}{\varepsilon_{r(0)}} = \frac{1}{[1+\alpha\varepsilon_0^3\varepsilon_{r(0)}^3E^2]^{1/3}} \quad (3)$$

where ε_0 is the dielectric constant of free space, $\varepsilon_{r(E)}$ and $\varepsilon_{r(0)}$ represent the dielectric constants (relative to the ε_0) under a bias field E and zero bias field, respectively, and the α is the phenomenological coefficient [25]. The pre-factor term of E^2, $\alpha\varepsilon_0^3\varepsilon_{r(0)}^3$, is defined as the field coefficient [21]. Fig. 8 shows the fitting plots of the dielectric constants measured in different cycles. For each sweep, the measured data under the bias field basically agree with the phenomenological framework. Like the case of the ceramic specimen, the dielectric nonlinearity of the thick film was found to be sensitive to the field history [10]. The sensitivity is related to the response of extrinsic polarizable entities under the bias field [26]. The polarization of the PNRs embedded in the paraelectric background of the thick film is regarded to be the main extrinsic polarization mechanism [10]. Moreover, the interfacial polarization may also contribute to the sensitivity.

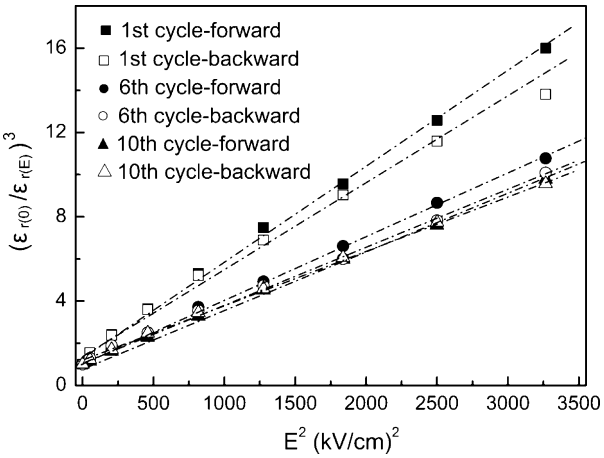

Fig. 8. Fitting plots to the Johnson relation for the dielectric constants of the thick film measured in different cycles of bias electric field sweep.

Fig. 9 shows the dielectric nonlinearity parameters of the thick film as a function of the cycle number. The tunability was determined at 57 kV/cm. The field coefficient and the phenomenological coefficient were calculated from the fitting to the Johnson relation. The dielectric constant, tunability and field coefficient varied with the cycle number in an identical manner (Fig. 9a–c), declining with the cycle number and tending to be somewhat saturated after six cycles. The identity is rational due to the correlation of the three parameters in physics [18,27]. By contrast, the phenomenological coefficient is basically independent of the field history (Fig. 9d). The independent behavior is logical because the phenomenological coefficient essentially, as an order parameter, reflects the contribution of the intrinsic polarization mechanism (i.e. lattice

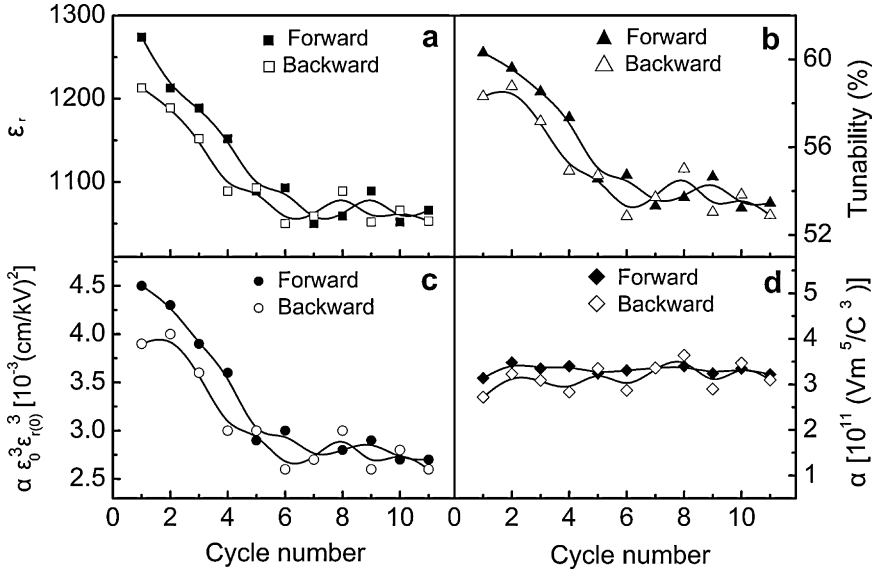

Fig. 9. Dielectric nonlinearity parameters of the thick film as a function of cycle number of bias electric field sweep: (a) dielectric constant, (b) tunability, (c) field coefficient and (d) phenomenological coefficient.

phonon polarization) to the dielectric nonlinearity for $Ba_{0.6}Sr_{0.4}TiO_3$ in paraelectric state [24–26]. This behavior, in turn, validates that the sensitivity of the dielectric nonlinearity to the field history (Fig. 8) is related with the extrinsic polarization mechanisms of the thick film.

In general, the evolution of the dielectric nonlinearity parameters of the thick film with the cycle number is consistent with that of the ceramic specimen [10]. Major inconsistency in the parameters between the two type specimens lies in the following two points. In the case of forward sweep, the tunability of the thick film degraded by about 12% after ten cycles. The degradation is less prominent in magnitude compared to that of the ceramic specimen, i.e., decaying by about 35% after eleven cycles. This comparison indicates a weakened field history dependence of the dielectric nonlinearity for the thick film. A possible explication may be that the porous microstructure of the thick film altered the bias field practically applied on the grains. On the other hand, the phenomenological coefficient α (around 3.2×10^{11} V m^5/C^3) of the thick film is larger by one order of magnitude than that (around 2.5×10^{10} V m^5/C^3) of the ceramic specimen [10]. The phenomenological coefficient is closely associated with the interaction of the titanium ions oscillating in an anharmonic potential [25]. It is argued that the presence of reduced titanium ions in the lattice is prone to enhancing the anharmonic interaction. This effect is considered responsible for the larger phenomenological coefficient of the thick film.

The trend ‘‘the higher the dielectric constant, the higher the tunability’’ has been validated for many dielectrics [2]. As afore-mentioned, regardless of an apparently lowered dielectric constant, the tunability of the thick film measured at about 20 kV/cm is comparable in magnitude with that of the ceramic specimen. The phenomenon can be qualitatively explained with respect to the phenomenological coefficient. The field coefficient, $\alpha\varepsilon_0^3\varepsilon_{r(0)}^3$, is consistent in physical meaning with the tunability, that is, characterizing the efficiency of applied bias field in depressing dielectric constant [21]. The large phenomenological coefficient of the thick film is believed to be the reason for its good tunability in the context of the apparently lowered dielectric constant.

4. Conclusions

$Ba_{0.6}Sr_{0.4}TiO_3$ thick films have been prepared by screen printing utilizing superfine powder derived from the citrate method. A cubic perovskite structure and a porous microstructure was detected for the thick film sintered at 1250 °C. The inspection on the dielectric properties for the thick film in comparison with dense ceramic specimen highlights an important role of the porous microstructure on the dielectric properties. The porous microstructure of the thick film led to a decreased dielectric constant, an increased dielectric loss and a reduced field history dependence of the dielectric nonlinearity. The increased dielectric loss of the thick film was explained with an appreciable interfacial polarization and an enhanced electric conduction. Reasonably good dielectric nonlinearity of the porous thick film is proposed to be due to its large phenomenological coefficient. At room temperature, the thick film exhibited a dielectric constant of 1270 and a dielectric loss of 1.4% at zero bias field and 10 kHz along with a tunability of 60% and a figure of merit of 43 at 57 kV/cm and 10 kHz.

Acknowledgements

This work was supported by the National Natural Science Foundation of China (Nos. 51072146 and 50932004), the Ministry of Education (Nos. 20100143110006 and 108092) and Hubei Provincial Science and Technology Department (No. 2011CDA057).

References

[1] L.C. Sengupta, S. Sengupta, Breakthrough advances in low loss, tunable dielectric materials, Mater. Res. Innovat. 2 (1999) 278–282.
[2] A.K. Tagantsev, V.O. Sherman, K.F. Astafiev, J. Venkatesh, N. Setter, Ferroelectric materials for microwave tunable applications, J. Electroceram. 11 (2003) 5–66.
[3] F. Zimmermann, M. Voigts, C. Weil, R. Jakoby, P. Wang, W. Menesklou, E. Ivers-Tiffee, Investigation of barium strontium titanate thick films for tunable phase shifters, J. Eur. Ceram. Soc. 21 (2001) 2019–2023.
[4] B. Su, J.E. Holmes, C. Meggs, T.W. Button, Dielectric and microwave properties of barium strontium titanate (BST) thick films on alumina substrates, J. Eur. Ceram. Soc. 23 (2003) 2699–2703.
[5] D. Zhang, W.F. Hu, C. Meggs, B. Su, T. Price, D. Iddles, M.J. Lancaster, T.W. Button, Fabrication and characterisation of barium strontium titanate thick film device structures for microwave applications, J. Eur. Ceram. Soc. 27 (2007) 1047–1051.
[6] R. Wu, P.Y. Du, W.J. Weng, G.R. Han, Preparations and dielectric properties of $Ba_{0.80}Sr_{0.20}TiO_3$/PbO–B_2O_3 thick films, Mater. Chem. Phys. 97 (2006) 151–155.
[7] T. Tick, J. Perantie, H. Jantunen, A. Unsimaki, Screen printed low-sintering-temperature barium strontium titanate (BST) thick films, J. Eur. Ceram. Soc. 28 (2008) 837–842.
[8] F. Zimmermann, M. Voigts, W. Menesklou, E.I. Tiffee, $Ba_{0.6}Sr_{0.4}TiO_3$ and $BaZr_{0.3}Ti_{0.7}O_3$ thick films as tunable microwave dielectrics, J. Eur. Ceram. Soc. 24 (2004) 1729–1733.
[9] X.F. Zhang, Q. Xu, Y.H. Huang, H.X. Liu, D.P. Huang, F. Zhang, Low-temperature synthesis of superfine barium strontium titanate powder by the citrate method, Ceram. Int. 36 (2010) 1405–1409.
[10] X.F. Zhang, Q. Xu, H.X. Liu, W. Chen, M. Chen, B.H. Kim, Field history dependence of nonlinear dielectric properties of $Ba_{0.6}Sr_{0.4}TiO_3$ ceramics under bias electric field: polarization behavior of polar nano-regions, Physica B 406 (2011) 1571–1576.
[11] K.L. Choy, S. Charojrochkul, B.C.H. Steele, Fabrication of cathode for solid oxide fuel cells using flame assisted vapour deposition technique, Solid State Ionics 96 (1997) 49–54.
[12] A. Feteira, D.C. Sinclair, I.M. Reaney, Y. Somiya, M.T. Lanagan, $BaTiO_3$-based ceramics for tunable microwave applications, J. Am. Ceram. Soc. 87 (2004) 1082–1087.
[13] S.J. Lee, K.Y. Kang, S.K. Han, Low-frequency dielectric relaxation of $BaTiO_3$ thin-film capacitors, Appl. Phys. Lett. 75 (1999) 1784–1786.
[14] D. O’Neill, R.M. Bowman, J.M. Gregg, Dielectric enhancement and Maxwell–Wagner effects in ferroelectric superlattice structures, Appl. Phys. Lett. 77 (2000) 1520–1522.
[15] X.F. Liang, Z.Y. Meng, W.B. Wu, Effect of acceptor and donor dopants on the dielectric and tunable properties of barium strontium titanate, J. Am. Ceram. Soc. 87 (2004) 2218–2222.
[16] Z. Li, H.Q. Fan, Polaron relaxation associated with the localized oxygen vacancies in $Ba_{0.85}Sr_{0.15}TiO_3$ ceramics at high temperatures, J. Appl. Phys. 106 (2009), 054102-1-5.

[17] W.H. Zhang, J.X. Zhang, Photoluminescence at room temperature in $Ba_{0.5}Sr_{0.5}TiO_3$ ceramics, J. Lumin. 131 (2011) 2307–2310.
[18] S.I Jang, H.M. Jang, Leakage-current characteristics of sol–gel-derived $Ba_{1-x}Sr_xTiO_3$ (BST) thin films, Ceram. Int. 26 (2000) 421–425.
[19] K.B. Jinesh, Y. Lamy, J.H. Klootwijk, W.F.A. Bestling, Maxwell–Wagner instability in bilayer dielectric stacks, Appl. Phys. Lett. 95 (2009), 122903-1-3.
[20] C. Ang, Z. Yu, High capacitor-temperature sensitivity and giant dielectric constant in $SrTiO_3$, Appl. Phys. Lett. 90 (2007), 202903-1-3.
[21] J.W. Liou, B.S. Chiou, DC Field dependence of the dielectric characteristics of doped $Ba_{0.6}Sr_{0.35}TiO_3$ with various grain sizes in the paraelectric state, Jpn. J. Appl. Phys. 36 (1997) 4359–4368.
[22] Y.Y. Zhang, G.S. Wang, T. Zeng, R.H. Liang, X.L. Dong, Electric field-dependent dielectric properties and high tunability of porous $Ba_{0.5}Sr_{0.5}TiO_3$ ceramics, J. Am. Ceram. Soc. 90 (2007) 1327–1330.
[23] M. Voigts, W. Menesklou, E.I. Tiffee, Dielectric properties and tunability of BST and BZT thick films for microwave applications, Integr. Ferroelectr. 39 (2001) 383–392.
[24] K.M. Johnson, Variation of dielectric constant with voltage in ferroelectrics and its application to parametric devices, J. Appl. Phys. 33 (1962) 2826–2831.
[25] J.W. Liou, B.S. Chiou, Effect of direct-current biasing on the dielectric properties of barium strontium titanate, J, Am. Ceram. Soc. 80 (1997) 3093–3099.
[26] C. Ang, Z. Yu, DC electric-field dependence of the dielectric constant in polar dielectric: multipolarization mechanism model, Phys. Rev. B 69 (2004), 174109-1-8.
[27] J.J. Zhang, J.W. Zhai, X.J. Chou, J. Shao, X. Lu, X. Yao, Microwave and infrared dielectric response of tunable $Ba_{1-x}Sr_xTiO_3$ ceramics, Acta. Mater. 57 (2009) 4491–4499.